Int J Adv Manuf Technol (2009) 43:1024–1034
DOI 10.1007/s00170-008-1783-z

ORIGINAL ARTICLE

Design and manufacture of plunge shaving cutter for shaving gears with tooth modifications

Jia-Hung Liu · Ching-Hua Hung · Shinn-Liang Chang

Received: 11 March 2008 / Accepted: 30 September 2008 / Published online: 29 October 2008

Abstract Gear plunge shaving is one of the most efficient ways to finish gears. It has been a challenge for a long time to design and manufacture a plunge shaving cutter to induce gear tooth modification. This paper proposes a method for designing plunge shaving cutters to manufacture gears with modifications analytically. By integrating B-spline interpolation, differential geometry, and design optimization, the goal is achieved. Efficiency is greatly improved by avoiding the traditional trial and error method.

Keywords Plunge shaving cutter · Gear tooth modification · B-spline interpolation · Design optimization

1 Introduction

Gears are the most important components in transmission systems. Modifications of gear teeth can accommodate errors and deformations encountered in the manufacture, assembly, and operation of gear pairs. Litvin [1] provided a double-crowned gear modified both in lead and in profile with improved transmission error. Wagaj and Kahraman [2] investigated the durability of helical gear affected by tooth modifications. Kahraman et al. [3] presented a gear wear model analyzing the influences of tooth modification.

Gear shaving is one of the most efficient and economical processes for gear finishing after hobbing or shaping. There are four basic shaving methods: Conventional/transverse, diagonal, and underpass shaving are composed of axial/longitudinal and radial infeeds, and the parameters can be optimized for better performances [4]. Plunge shaving is the most advanced gear finishing technique, which only needs radial infeed. Its advantages include increased productivity, accuracy, long tool life, and a simple machine structure [5]. The basic meshing condition of 3D crossed-axis helical gear pair was first derived by Litvin [6], and it has been widely adopted as the fundamental assumption for simulation of gear shaving.

In recent years, how to induce gear tooth modification by shaving has become an important subject of research. Chang et al. [7] and Hung et al. [8] derived the mathematical model of traditional shaving machine and investigated the influences of parameters on tooth lead modifications. Litvin et al. [9] proposed a method for shaving gears with double crowning by computer numerical control (CNC) shaving machine. For shaving methods other than plunge shaving, the gear tooth modification is accomplished by tooth modifications of the shaving cutter and the coordinated motions between cutter and gear. For the plunge shaving method, however, it only depends on the surface geometry of the plunge shaving cutter. Traditionally, the cutter surface geometry results from a cutter re-sharpening machine by trial and error.

Focusing on the surface geometry of shaving cutter, what is really significant is precision of the region

J.-H. Liu · C.-H. Hung
Mechanical Engineering Department,
National Chiao Tung University,
EE507, 1001 Ta Hsueh Rd.,
Hsinchu 30010 Taiwan, Republic of China

S.-L. Chang (✉)
Institute of Mechanical and Electro-mechanical Engineering,
National Formosa University,
Room 529, Building 2, The New Campus, No.64, Wunhua Rd.,
Huwei Township,
Yunlin County 632 Taiwan, Republic of China
e-mail: changsl@nfu.edu.tw

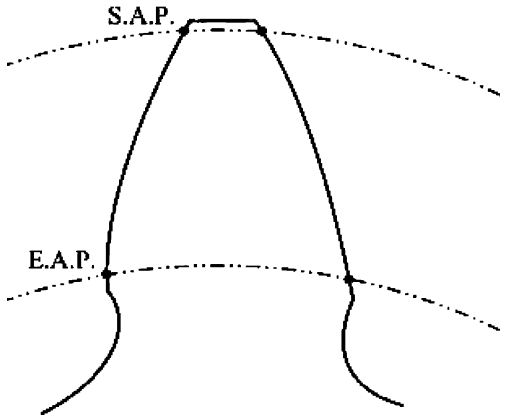

Fig. 1 SAP and EAP of a shaving cutter tooth

between start of active profile (SAP) and end of active profile (EAP) as shown in Fig. 1. In gear shaving, EAP of cutter tooth shaves the gear tooth tip, while SAP shaves the gear tooth root. Koga et al. [10] explored the errors in the cutter's tooth profile that resulted from the grinding machine setup. Hsu [11] investigated the topographic error of cutters from a re-sharpening machine for shaving involute gears. Radzevich [12–13] proposed a methodology for calculating the parameters of the plunge shaving cutter and the respective form grinding wheel from measured discrete points of the modified gear. Nevertheless, without an analytical description of the modified gear and the plunge shaving cutter, further investigations are still limited.

Numerical approximation and interpolation are commonly used to construct an analytical description of discrete data points. Piegl and Tiller [14] provided basic theories for numerical approximations and interpolations. Wang et al. [15] studied the geometric relationship and conjugate motion of digital gear tooth surface composed of discrete points. Barone [16] used B-spline curve fitting and swept surface to model gears with profile modifications. In this paper, the analytical description of the gear with tooth modifications is first constructed by B-spline surface fitting. Then, the grinding wheel profile is parameterized and optimized for minimizing the surface deviations of theoretical and ground (from re-sharpening machine) tooth surfaces of the plunge shaving cutter. Efficiency is greatly improved by avoiding the traditional trial and error method, and the constructed mathematical model of plunge shaving cutter can be further utilized as the base for extending researches.

2 Surface interpolation of the modified gear tooth surface

To integrate the modified gear tooth surfaces into the analytical process, especially for those with both lead and profile modifications, B-spline surface interpolation is

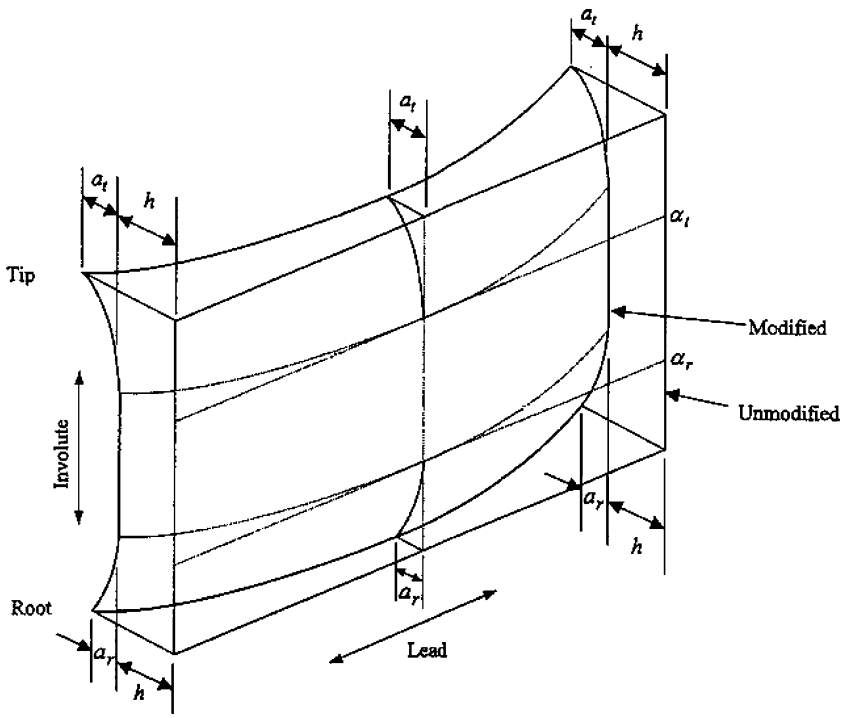

Fig. 2 Model of gear tooth modifications [2]

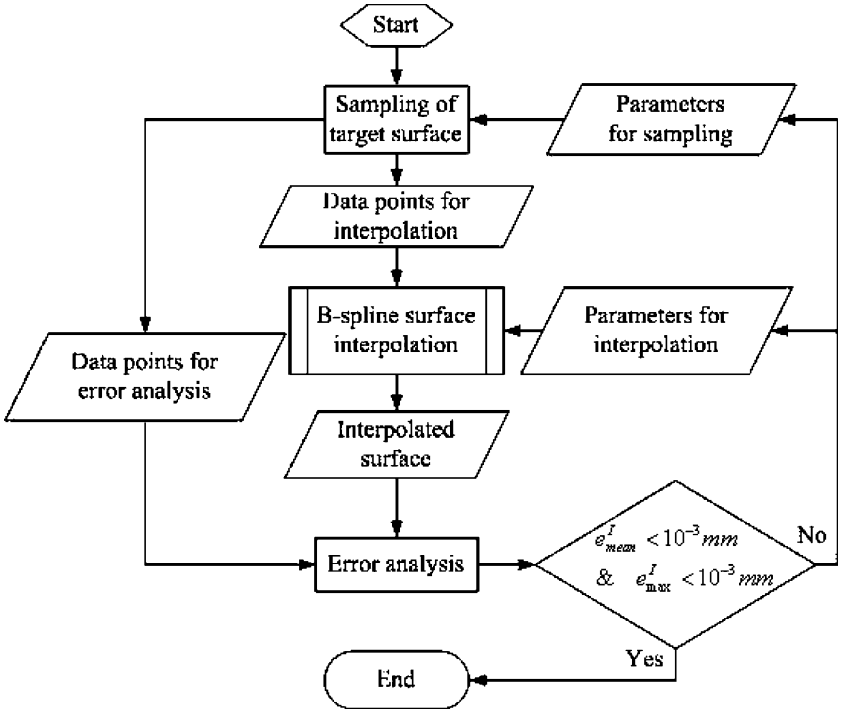

Fig. 3 Flowchart of interpolation error analysis

selected for its ease of manipulation. In practice, the sampling points of the modified surface can be obtained by coordinate measuring machine or from other sources. In this paper, for studying purposes, the most commonly used numerical model is adopted for generation of interpolating points: The tooth flank is modified in profile (root to tip) and lead (side to side) directions independently as shown in Fig. 2 [2]. The magnitude at the tip a_t and the gear roll angle at the start α_t define the boundaries of the tip relief. Between these two points, the profile follows a linear trajectory. Similarly, the magnitude a_r and the starting roll angle α_r define the starting point of a root modification. The amount of lead crowning is denoted by h.

A B-spline representation enables the simulation of surface irregularities and the control of small tooth geometric modifications, such as rounding and reliving. Given a grid of sampling points $D_{k,\ell}$ ($0 \le k \le m$ and $0 \le \ell \le n$) and orders p and q (degrees $p-1$ and $q-1$), it can be represented as below [14]:

$$D_{k,\ell} = \sum_{i=0}^{m} \sum_{j=0}^{n} N_{i,p}(s_k) N_{j,q}(t_\ell) P_{i,j} \tag{1}$$

where s_k's and t_l's are the chosen parameter values; $N_{i,p}$ (s_k) ($N_{j,q}$ (t_ℓ)) is the i-th (j-th) B-spline basis function of order p (q); and $p_{i,j}$'s ($0 \le i \le m$ and $0 \le j \le n$) are the control points. Once the numbers of sampling points m and n are selected, then the B-spline orders p and q are limited by Eq. 2:

$$p \ge \frac{3m+1}{m+1}, \quad q \ge \frac{3n+1}{n+1} \tag{2}$$

that is, $p \ge 3$ and $q \ge 3$.

Table 1 Basic data of the target surfaces

Gear data	
Diameter of base circle d_{b2}	119.618 mm
Diameter of addendum circle d_{add2}	126.71 mm
Diameter of root circle d_{r2}	119.33 mm
Diameter of pitch circle d_{p2}	123.915 mm
Normal pressure angle in pitch circle α_{pn2}	14.5°
Face width f_{w2}	18 mm
Gear tooth number Z_2	79
Helix angle in pitch circle β_{p2}	17°
Normal circular tooth thickness s_{pn2}	2.32mm

Table 2 Data of gear tooth modifications of the target surfaces

Parameter	Σ_{S2}	Σ_{L2}	Σ_{D2}
a_t	0	0	6e−3 mm
α_t	N/A	N/A	31.8°
a_r	0	0	6e−3 mm
α_r	N/A	N/A	28.2°
h	0	6e−3 mm	6e−3 mm

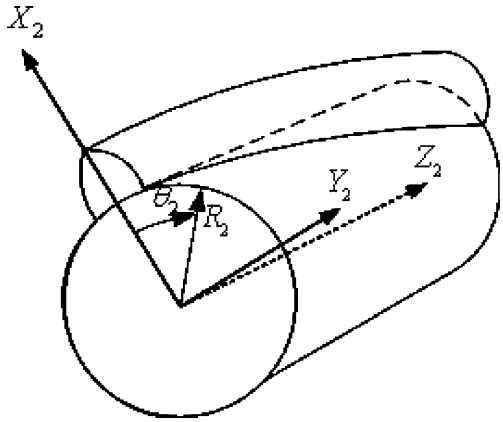

Fig. 4 Cylindrical coordinate used for sampling data points

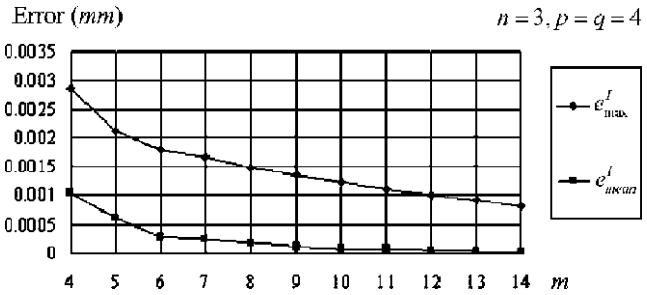

Fig. 5 Interpolation error of $\sum^I_{D2}$ by changing m ($n = 3$, $p = q = 4$)

Solving Eq. 1, $P_{i,j}$'s can be obtained, and the interpolated B-spline surface $\sum^I_2$ can be represented as follows:

$$\sum\nolimits^I_2 (u,v) = \sum_{i=0}^{m}\sum_{j=0}^{n} N_{i,p}(u)N_{j,q}(v)P_{i,j} \tag{3}$$

where u and v denote the surface parameters; 2 denotes the surface of gear tooth; and I denotes the surface obtained by interpolation.

B-spline interpolation can be implemented using the MATLAB Spline Toolbox by specifying a set of data points and either knot sequences or orders of the interpolated surface. The process of obtaining the B-spline surface is illustrated in Fig. 3. For example, to interpolate the gear tooth surfaces described in Tables 1 and 2, including three target gear tooth surfaces (standard $\sum_{S2}$, lead crowned $\sum_{L2}$, and double crowned $\sum_{D2}$), three sets of sampling points must be acquired from the model shown in Fig. 2. In order to obtain gridded data points for interpolations, the target surfaces are sampled in the cylindrical coordinate system (represented by R_2, θ_2, and Z_2) for the nature of the cylindrical gear, as shown in Fig. 4.

By specifying the number of sampling points m and n in the R_2 and Z_2 coordinates as well as the respective orders p and q, three interpolated tooth surfaces can be expressed as $\sum^I_{S2}(R_2,Z_2)$, $\sum^I_{L2}(R_2,Z_2)$, and $\sum^I_{D2}(R_2,Z_2)$. Three sets of data points (30×30 in R_2 and Z_2 coordinates for each set) are also sampled from the three target surfaces for error analysis. The interpolation error E^I is defined as a 30×30 matrix composed of values of arc length between the respective points (with the same values of radius and at the same axial cross-section) uniformly sampled from the target surface $\sum_2$ and the interpolated surface $\sum^I_2$. Each element $e^I_{i,j}$ of E^I can be expressed as:

$$e^I_{i,j} = r_{i,j}\left(\tan^{-1}\left(\frac{y_{i,j}}{x_{i,j}}\right) - \tan^{-1}\left(\frac{y^I_{i,j}}{x^I_{i,j}}\right)\right), \quad i,j = 1,2,\ldots,30 \tag{4}$$

where $r_{i,j}$ denotes the value of radius; $x_{i,j}$, $y_{i,j}$, and $x^I_{i,j}$, $y^I_{i,j}$ denote the points on $\sum_2$ and $\sum^I_2$, respectively, and the maximum $e^I_{\max}$ and the mean e^I_{mean} can be obtained.

Based on the error analysis in this section, E^I is not sensitive at all to the parameters in the Z_2 coordinates, including n and q. Even with lead modifications, the non-linearity remains quite small compared with that caused by profile modifications. Table 3 presents six conditions of $\sum^I_{S2}$. Increasing m and p improve the values of e^I_{mean} and

Table 3 Conditions and errors of B-spline surface interpolation $\left(\sum^I_{S2}\right)$

Parameter	Condition					
	1	2	3	4	5	6
m (R_2 coordinate)	3	4	4	5	5	5
n (Z_2 coordinate)	3	3	3	3	3	3
p (R_2 coordinate)	3	3	4	3	4	4
q (Z_2 coordinate)	3	3	3	3	3	4
$e^I_{\text{mean}}(10^{-3}\text{mm})$	9.805	1.721	1.193	0.645	0.185	0.185
$e^I_{\max}(10^{-3}mm)$	15.6745	4.55	1.795	1.8539	0.0679	0.0679

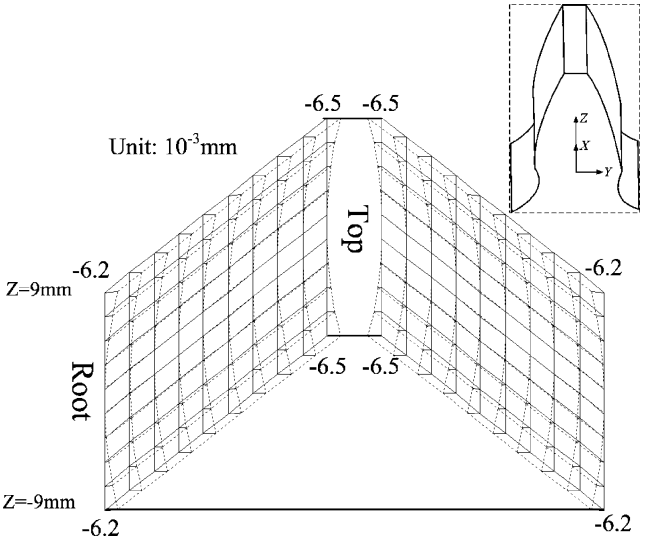

Fig. 6 Validations of interpolated surfaces ($\sum_{S2}^{I}$ vs. $\sum_{L2}^{I}$)

$e_{\max}^{I}$, which are commonly required to be less than 10^{-3} mm. Although the errors are the same in conditions 5 and 6, the parameters in condition 6 are preferable for higher differentiability. Errors of surface $\sum_{L2}^{I}$ are similar to that of $\sum_{L2}^{I}$. Nevertheless, for surface $\sum_{D2}^{I}$, under conditions similar to condition 6, m must increase to 14, as shown in Fig. 5, because of higher non-linearity due to profile modifications.

The interpolated surfaces $\sum_{L2}^{I}$and $\sum_{D2}^{I}$ are compared with $\sum_{S2}^{I}$ for validations as shown in the topographic charts (Figs. 6 and 7). The topographic errors between top and root on the left and right tooth flanks are calculated for

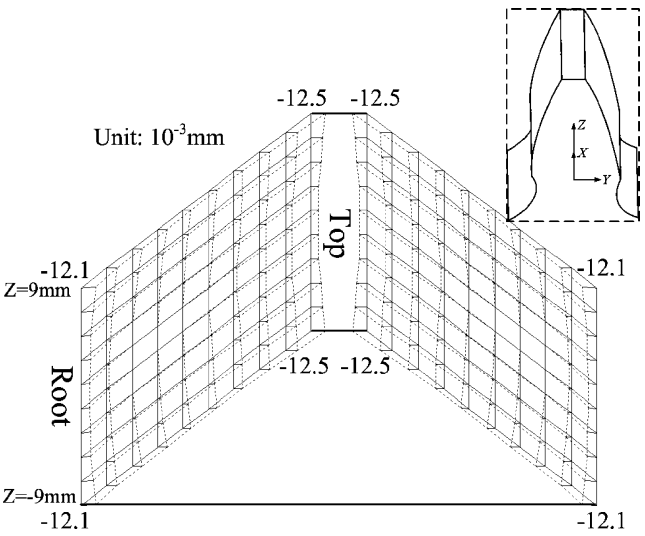

Fig. 7 Validations of interpolated surfaces ($\sum_{S2}^{I}$ vs. $\sum_{D2}^{I}$)

points of specific radiuses and Z cross-sections. $\sum_{S2}^{I}$ is presented in straight solid lines as the base of comparison, while $\sum_{L2}^{I}$ and $\sum_{D2}^{I}$ are presented in dashed lines. In Fig. 6, $\sum_{L2}^{I}$ is shown with lead modification only, and in Fig. 7, $\sum_{D2}^{I}$ is shown with both lead and profile modifications. Note that the values of the topographic differences are all represented in arc length.

3 Topographic errors of gear plunge shaving cutter

The tooth surface of the shaving cutter is usually finished last using a cone-grinding wheel on the shaving cutter re-sharpening machine. Because the topographic accuracy of the plunge shaving cutter maps directly onto the work gear, it is important to identify the topographic error of the ground tooth surfaces $\sum_{S1}^{G}$, $\sum_{L1}^{G}$, and $\sum_{D1}^{G}$ in comparison to the theoretical $\sum_{S1}^{T}$, $\sum_{L1}^{T}$, and $\sum_{D1}^{T}$. Here, 1 denotes the surface of shaving cutter tooth; G and T denote the surfaces derived from the re-sharpening machine and the interpolated surfaces, respectively.

The basic meshing condition for the crossed helical gear set [6] is used to calculate the basic geometric data for the shaving cutter. It needs the following eight basic items: the tooth number Z_1, the normal circular tooth thickness s_{pn1}, the helix angle β_{p1} of the shaving cutter; the tooth number Z_2, the normal circular tooth thickness s_{pn2}, the helix angle β_{p2} of the work gear; and the normal module m_{pn} and pressure angle α_{pn} of the shaving cutter and work gear. Figure 8 shows the coordinate system of the CNC shaving machine [11]. Considering coordinate transformation

$$\begin{aligned} \boldsymbol{r}_1 &= \begin{bmatrix} x_1 & y_1 & z_1 & 1 \end{bmatrix}^T = \mathbf{M}_{12}(\phi_2)\boldsymbol{r}_2(R_2, Z_2) \\ \boldsymbol{n}_1 &= \begin{bmatrix} n_{x1} & n_{y1} & n_{z1} \end{bmatrix}^T = \mathbf{L}_{12}(\phi_2)\boldsymbol{n}_2(R_2, Z_2) \end{aligned} \tag{5}$$

and meshing equation

$$f(R_2, Z_2, \phi_2) = \boldsymbol{n}_h \cdot \boldsymbol{v}_h^{(12)} = 0 \tag{6}$$

simultaneously, the theoretical tooth surface of shaving cutters $\sum_{S1}^{T}$, $\sum_{L1}^{T}$, and $\sum_{D1}^{T}$ can be derived from surfaces $\sum_{S2}^{I}$, $\sum_{L2}^{I}$, and $\sum_{D2}^{I}$. $\mathbf{M}_{12}$ and $\mathbf{L}_{12}$ are matrices for transforming position and unit normal vectors ($\boldsymbol{r}_2$ and $\boldsymbol{n}_2$) of surfaces $\sum_{S1}^{T}$, $\sum_{L1}^{T}$, and $\sum_{D1}^{T}$ from coordinate system S_2 (gear) to S_1 (shaving cutter), and $v_h^{(12)}$ denotes the vector of relative velocity on auxiliary coordinate system S_h.

Likewise, as shown in Fig. 9, the ground surfaces of shaving cutters $\sum_{S1}^{G}$, $\sum_{L1}^{G}$, and $\sum_{D1}^{G}$ can be obtained by coordinate transformations from S_g (grinding wheel) to S_s (shaving cutter)

$$\begin{aligned} \boldsymbol{r}_s &= \begin{bmatrix} x_s & y_s & z_s & 1 \end{bmatrix}^T = \mathbf{M}_{sg}\boldsymbol{r}_g \\ \boldsymbol{n}_s &= \begin{bmatrix} n_{xs} & n_{ys} & n_{zs} \end{bmatrix}^T = \mathbf{L}_{sg}\boldsymbol{n}_g \end{aligned} \tag{7}$$

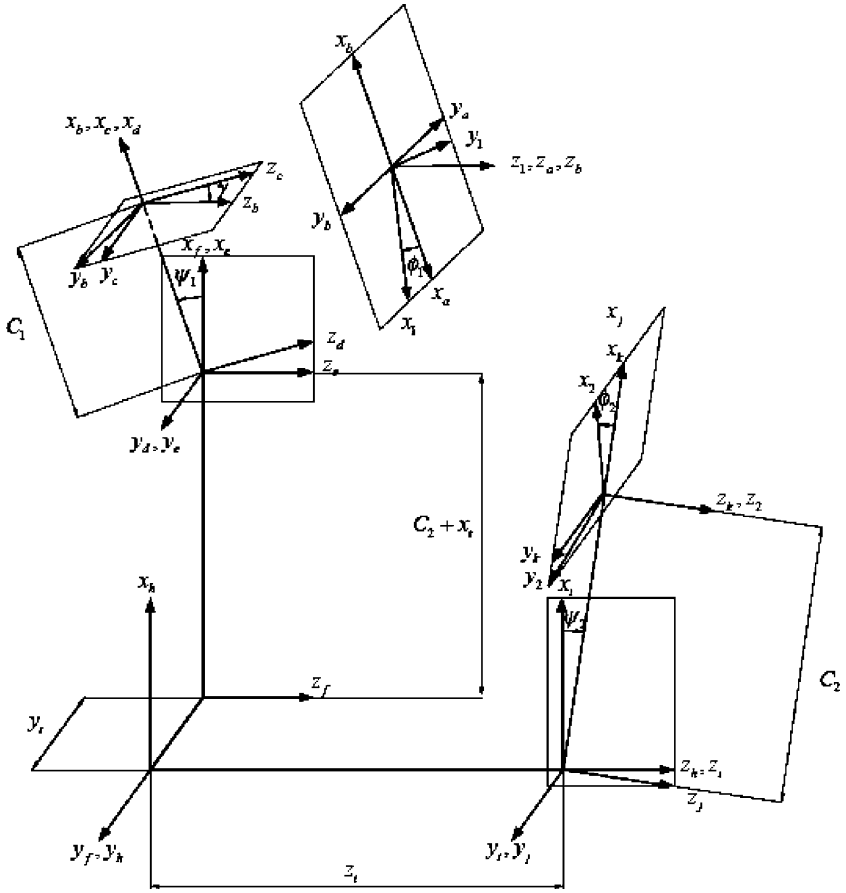

Fig. 8 Coordinate systems of gear shaving machine [10]

and the meshing equation

$$g\left(u_g, \theta_g, \phi\right) = \boldsymbol{n}_m \cdot \boldsymbol{v}_m^{(\mathrm{sg})} = 0 \tag{8}$$

An example is provided for illustration.

Example 1 For interpolated gear tooth surfaces $\sum_{S2}^{I}$ and $\sum_{D2}^{I}$ (see Tables 1 and 2), the corresponding data of plunge shaving cutter and grinding wheel are presented in Tables 4. Obtaining theoretical tooth surfaces $\sum_{S1}^{T}$ and $\sum_{D1}^{T}$ as well as ground tooth surfaces $\sum_{S1}^{G}$ and $\sum_{D1}^{G}$ through Eqs. 5, 6, 7, and 8, the topographic errors are calculated by

$$e_{i,j}^{\mathrm{Topo}} = r_{i,j}\left(\tan^{-1}\left(\frac{y_{i,j}^{T}}{x_{i,j}^{T}}\right) - \tan^{-1}\left(\frac{y_{i,j}^{G}}{x_{i,j}^{G}}\right)\right), \tag{9}$$

$$i = 1, 2 \ldots 5, j = 1, 2, \ldots, 9$$

and illustrated in Figs. 10 and 11 by 5×9 grids of specified radiuses and Z cross-sections, in which theoretical surfaces are presented in straight solid lines, while the corresponding ground ones are shown in dashed lines. From SAP to EAP of the cutter tooth, errors between $\sum_{D1}^{T}$ and $\sum_{D1}^{G}$ (Fig. 11) are less than those between $\sum_{S1}^{T}$ and $\sum_{S1}^{G}$ (Fig. 10). This is because of the nature of a grinding wheel with cone angle; that is, it presents a parabolic shape on the pitch line of a shaving cutter tooth, so that a specific amount of lead modification can be compensated.

4 Design optimization of the cone-grinding wheel

Compared with the setting parameters of the shaving cutter re-sharpening machine, the cone angle θ_c of the grinding wheel results in more influences on topographic errors of the final product. Traditionally, θ_c is modified back and forth for the desired accuracy, which is time-consuming. In this section, two examples are provided for illustrating design optimization by adjusting θ_c (Example 2) and the profile of the grinding wheel (Example 3).

Example 2 The objective of this example is to minimize the topographic errors between the theoretical tooth surface and the ground one. The flowchart is shown in Fig. 12, and the process is integrated by the MATLAB Optimization Toolbox. The problem is formulated as:

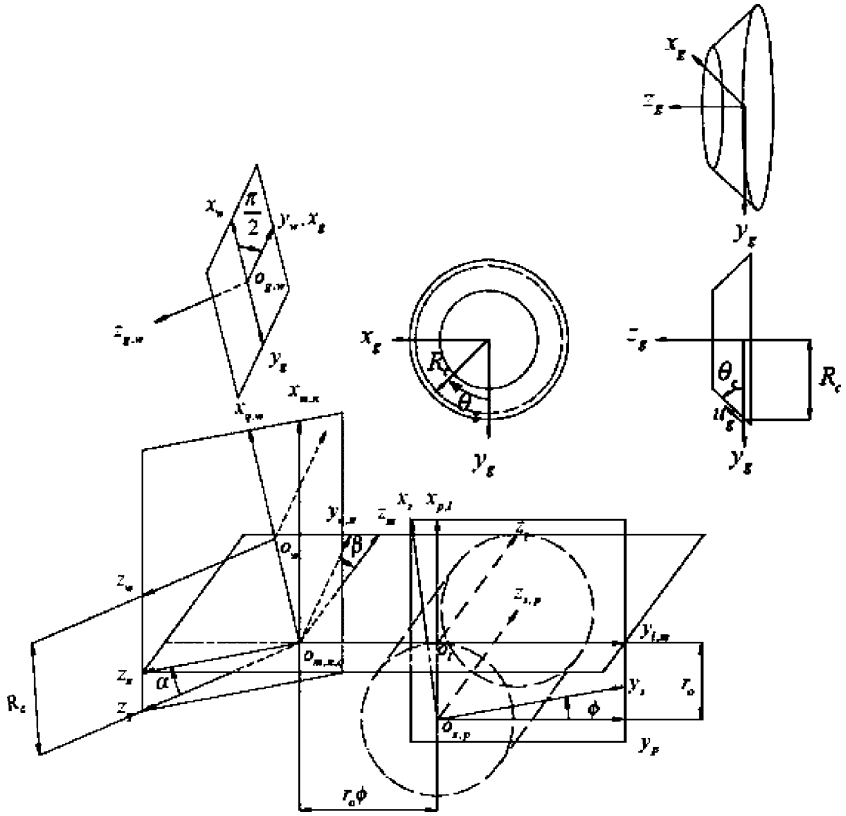

Fig. 9 Coordinate systems of shaving cutter re-sharpening machine [10]

find θ_c that

minimizes $\sum_{i=1}^{5}\sum_{j=1}^{9} e_{i,j}^{\text{Topo}}(\theta_c)$

subject to $e_{i,j}^{\text{Topo}} < 10^{-3}$mm, i=1,2,...,5, j=1,2,...,9,

and $1° \le \theta_c \le 30°$.

Considering 45 inequality constraints and one boundary constraint, the design variable θ_c is modified iteratively to obtain the optimum of topographic error. The process of calculating $e_{i,j}^{\text{Topo}}$ based on θ_c is considered as $e_{i,j}^{\text{Topo}}(\theta_c)$, and the sequential quadratic programming algorithm is adopted, where information of finite difference is used instead of gradients. For standard surfaces $\sum_{S1}^{T}$ and $\sum_{S1}^{G}$ shown in Fig. 13, the topographic errors are minimized when θ_c is modified from 10° (initial value) to 1° (optimum value),

Table 4 Data of cutter and grinding wheel for Example 1

Plunge shaving cutter	
Normal circular tooth thickness s_{pn1}	2.464 mm
Tooth number Z_1	139
Helix angle in pitch circle β_{p1}	20°
Face width f_{w1}	20 mm
Diameter of start of active profile (SAP)	225.922 mm
Diameter of end of active profile (EAP)	219.537 mm
Operating center distance E_o	173.04 mm
Operating crossed angle γ_o	3.002°
Grinding wheel and grinding machine	
Operating cone pitch radius R_c	350 mm
Cone angle θ_c	10°
Pressure angle α	4.675°
Operating radius r_o	111.03 mm

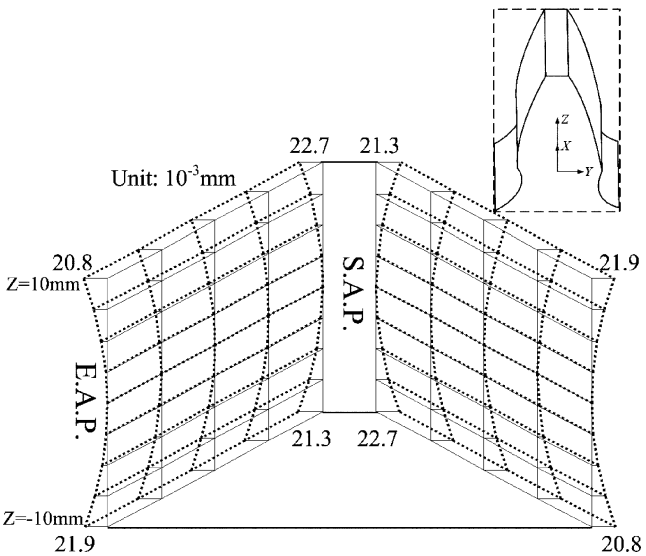

Fig. 10 Topographic errors between theoretical and ground shaving cutter tooth surfaces ($\sum_{S1}^{T}$ vs. $\sum_{S1}^{G}$)

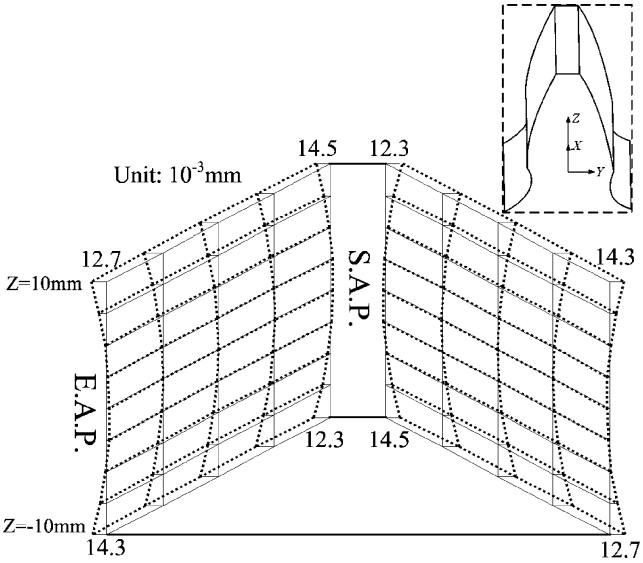

Fig. 11 Topographic errors between theoretical and ground shaving cutter tooth surfaces ($\sum_{D1}^{T}$ vs. $\sum_{D1}^{G}$)

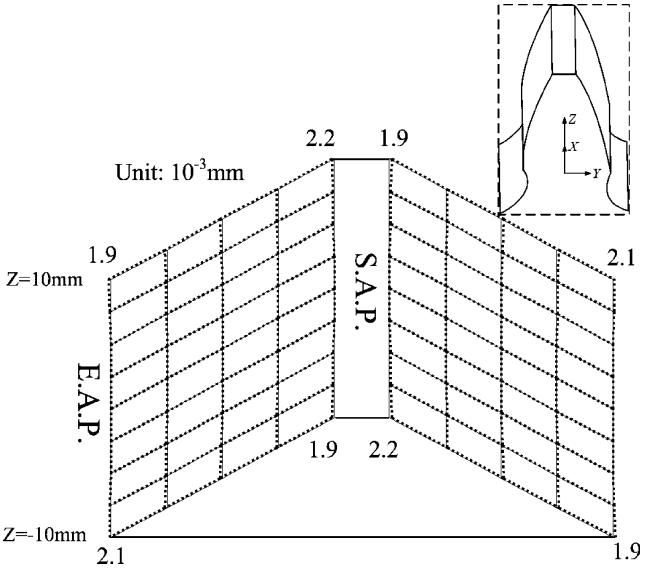

Fig. 13 Topographic errors between theoretical and ground shaving cutter tooth surfaces optimized by θ_c ($\sum_{S1}^{T}$ vs. $\sum_{S1}^{G}$)

which is active for the boundary constraint $1°\leq\theta_c\leq30°$. In practice, it is very difficult to make a grinding wheel with cone angle less than 1° so that the topographic error cannot be improved any more by only adjusting θ_c. For double-crowned tooth surfaces $\sum_{D1}^{T}$ and $\sum_{D1}^{G}$, the errors are still large at SAP and EAP (Fig. 14) due to profile modifications. To eliminate the errors, the profile of the grinding wheel also needs to be modified.

Example 3 Based on Fig. 9, the profile of grinding wheel is parameterized as shown in Fig. 15. Coordinate system S_g' is attached to the unmodified profile. Within the effective length L_A+L_A (L_A=4.2 mm, L_B=5.5 mm), the profile with four sections are defined by w_A, h_A, w_B, and h_B. Represented in S_g', the four points A_2, A_1, B_1, and B_2 are fitted by a B-spline curve with order 4. To improve the topographic errors between $\sum_{D1}^{T}$ and $\sum_{D1}^{G}$, the process of optimization is divided into two levels. The problem formulation for level 1: find θ_c

that minimizes $\sum_{j=1}^{9} e_j^{\text{Topo}}(\theta_c)$ on the pitch line of tooth surface

subject to $e_j^{\text{Topo}} < 10^{-3}$mm, j=1,2, …, 9 on the pitch line of tooth surface,

and $0.5°\leq\theta_c\leq30°$.

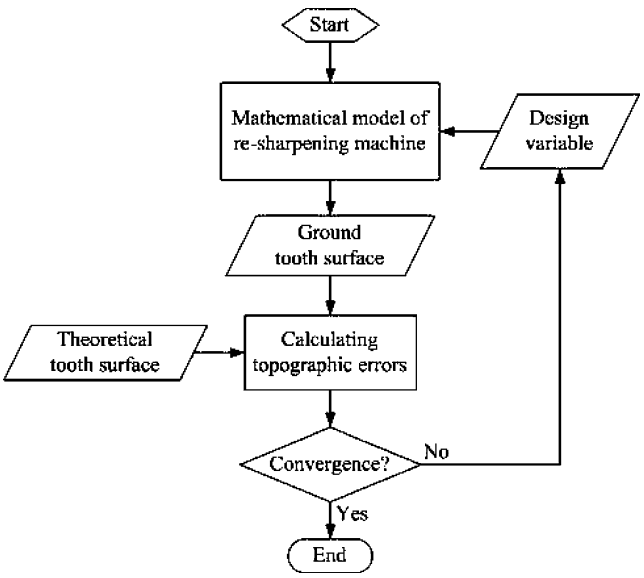

Fig. 12 Flowchart of design optimizations of the cone grinding wheel

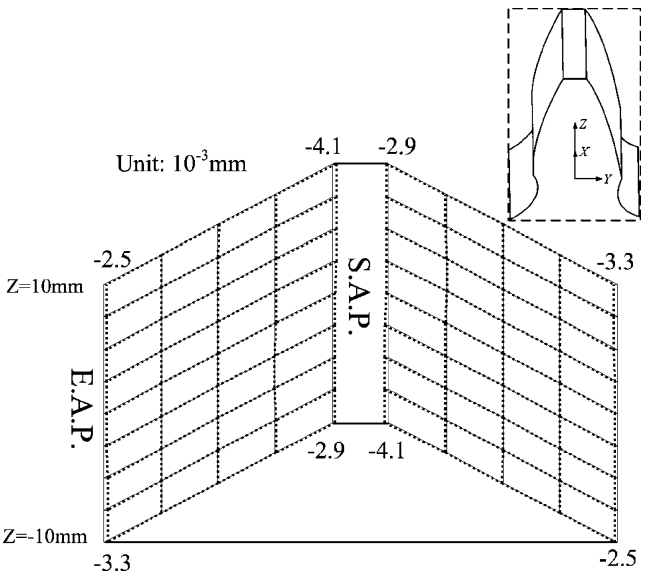

Fig. 14 Topographic errors between theoretical and ground shaving cutter tooth surfaces optimized by θ_c ($\sum_{D1}^{T}$ vs. $\sum_{D1}^{G}$)

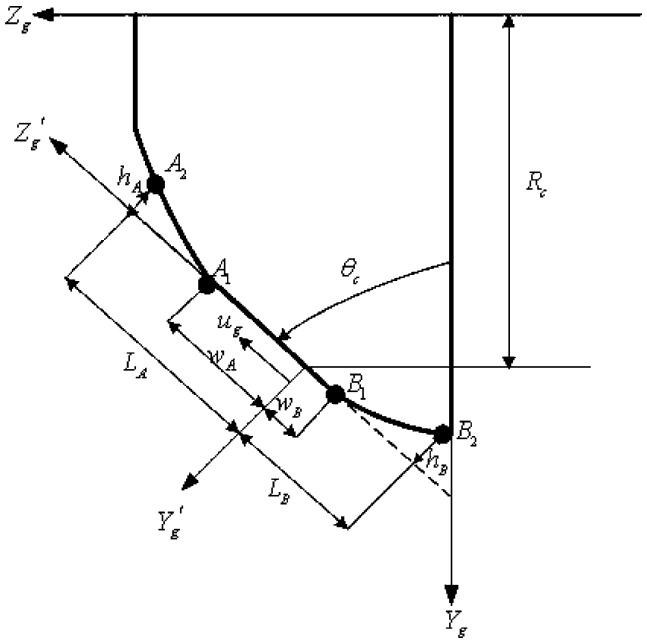

Fig. 15 Parameterized profile of grinding wheel for optimization

The first level converges efficiently to θ_c=2.382° and the problem formulation of level 2:
find $\mathbf{x}=[w_A, h_A, w_B, h_B]$

that minimizes $\sum_{i=1}^{5}\sum_{j=1}^{9} e_{i,j}^{\text{Topo}}(\mathbf{x})$

subject to $e_{i,j}^{\text{Topo}} < 10^{-3}$mm, i=1,2, …,5, j=1,2, …, 9

and $10^{-14}<w_A<L_A-10^{-4}$;$0<h_A<3$;$10^{-4}<w_B<L_B-10^{-4}$;$0<h_B<3$ (unit, mm).

Following the similar concepts of programming in Example 2, the optimum design is presented in Table 5.

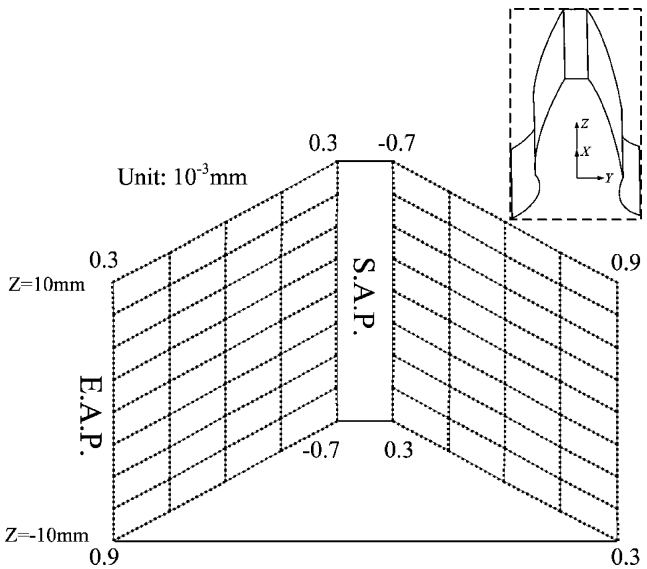

Fig. 16 Topographic errors between theoretical and ground shaving cutter tooth surfaces by profile optimization ($\sum_{D1}^{T}$ vs. $\sum_{D1}^{G}$)

Table 5 Results of the second level optimization in Example 3

	Initial design	Optimum design (mm)
w_A	0.1	0.561
h_A	0	0.056
w_B	0.1	0.538
h_B	0	0.235

The profile of the grinding wheel is considered straight sided initially. When it reaches optimum, the profile is modified for conjugation to the shaving cutter. The topographic errors between $\sum_{D1}^{T}$ and $\sum_{D1}^{G}$ are shown in Fig. 16, where the errors are all controlled below 10^{-3} mm.

Experiment of Example 3 has been conducted for validation of the proposed method. Figure 17 shows the plunge shaving cutter with an enlarged view of the cutting edges. Figure 18 shows the pre-shaved gear with an enlarged view of the obviously scalloped tooth surfaces measured as shown in Fig. 19. Firstly, the shaving cutter is ground by the grinding wheel on the re-sharpening machine (Fig. 20), on which the grinding wheel are modified first by the dresser according to the calculated cone angle and profile parameters. Then, the gear is plunge shaved on NACHI shaving machine with the setup shown in Fig. 21. Materials of gear and cutter are SCM435 and M2, and the operating speed as well as plunge infeed are set as 150 rpm and 1 mm/min, respectively. The shaved gear is measured as shown in Fig. 22, and the mean values of tooth modification are recorded in Table 6. It is found that:

1. Most of the scallops are eliminated and the surface roughness is greatly improved, especially in the lead direction;
2. The amounts of modifications, though with little deviations, are close to the original design values;

Fig. 17 Plunge shaving cutter used in the experiment

Fig. 18 Pre-shaved gear used in the experiment

3. Larger modifications are induced on left flank compared with right flank; this is because the left flank is the driving one in shaving with larger cutting force;
4. Efficiency is greatly improved by adopting the proposed method instead of trial and error.

5 Conclusions

Design and manufacture of the plunge-typed gear shaving cutters has always been a challenge, especially for those used to manufacture gears with modifications. This paper proposes a method for design and manufacture of the plunge shaving cutter for gears with modifications analytically, rather than trial and error. By integrating B-spline interpolation, differential geometry, and design optimiza-

Fig. 20 Plunge shaving cutter ground by the grinding wheel of the re-sharpening machine

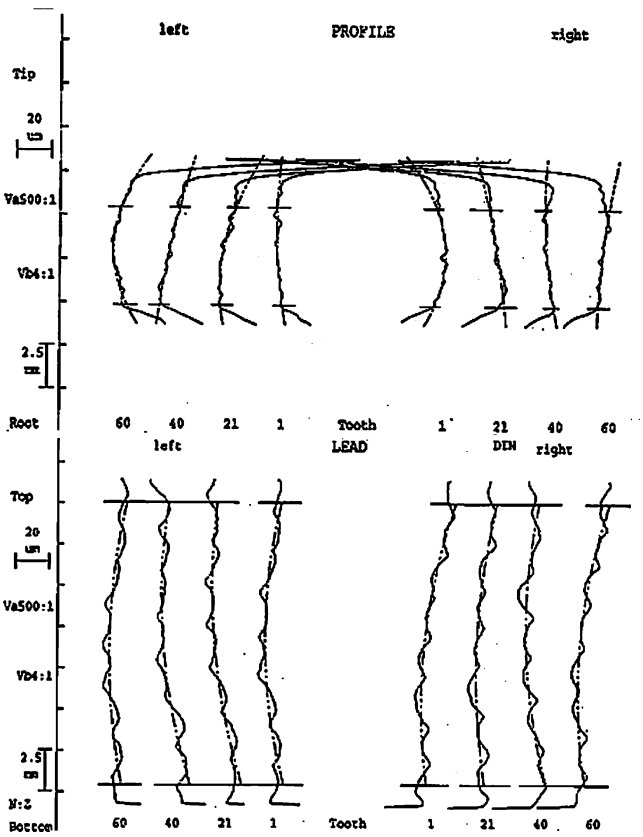

Fig. 19 Measured data of the pre-shaved gear used in the experiment

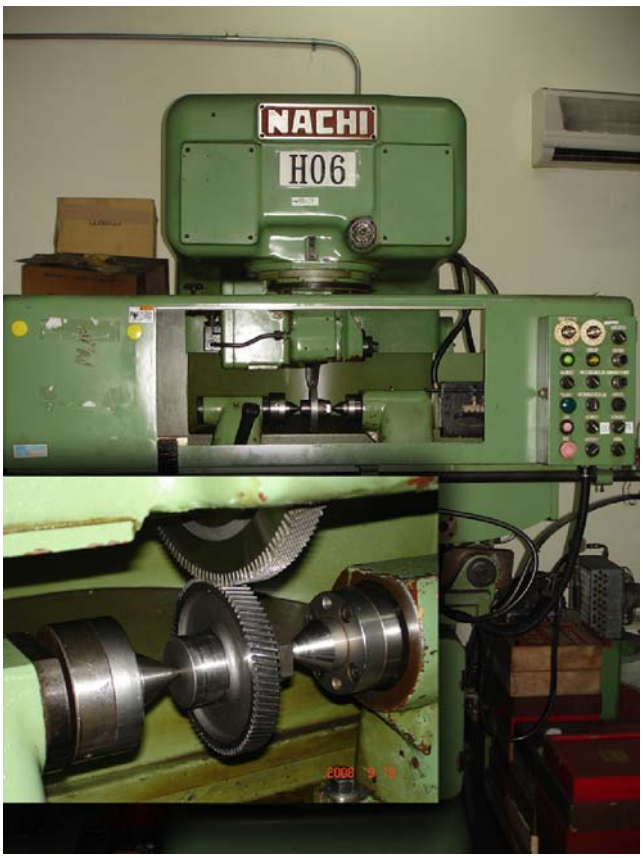

Fig. 21 NACHI shaving machine used in the experiment

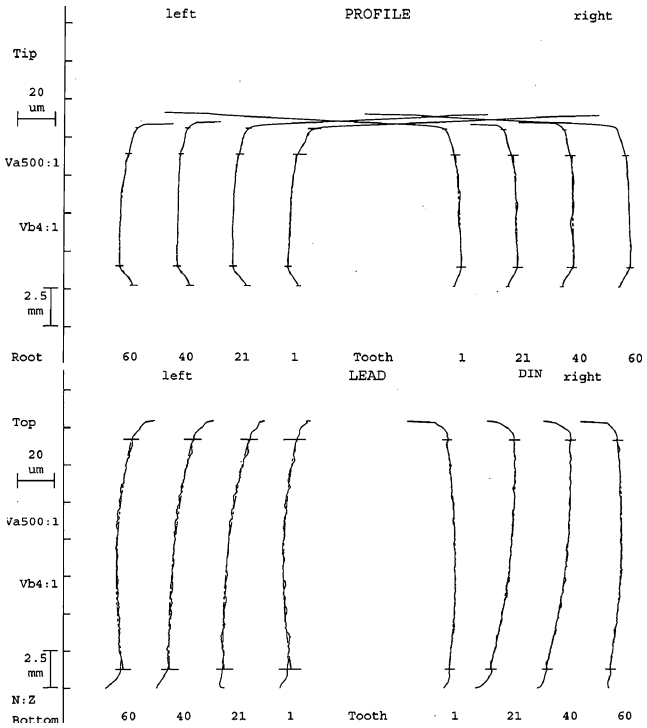

Fig. 22 Measured data of the shaved gear after the experiment

tion, the goal is achieved. To interpolate gears with both lead and profile modifications (double crowned), more sampling points are needed in the radial direction. In manufacturing a shaving cutter, the lead modification can be compensated by adjusting the cone angle, and the profile modification can be implemented by modifying the profile of the grinding wheel. Efficiency is greatly improved by avoiding traditional trial and error method through the proposed one. Besides, an analytical description of the modified gear tooth surface is also constructed, which can be utilized for extending research on serrations and shaving process.

Table 6 Achieved tooth modifications of gear after the experiment for validating Example 3

	Left flank (10^{-3} mm)		Right flank (10^{-3} mm)	
	Design	Real	Design	Real
Profile				
Tip	6	6.9	6	5.2
Root	6	6.1	6	5.1
Lead	6	5.8	6	5.4

Acknowledgment The authors wish to acknowledge the help from Luren Precision Co., Ltd. for providing all the necessities for the experiments.

References

1. Litvin FL (2001) Helical and spur gear drive with double-crowned pinion tooth surfaces and conjugated gear tooth surfaces. United States Patent, Patent no. US6205879
2. Wagaj P, Kahraman A (2002) Influence of tooth profile modification on helical gear durability. J Mech Des 124:501–510. doi:10.1115/1.1485289
3. Kahraman A, Bajpai P, Anderson NE (2005) Influence of tooth profile deviations on helical gear wear. J Mech Des 127:656–663. doi:10.1115/1.1899688
4. Radzevich SP (2007) Diagonal shaving of an involute pinion: optimization of the geometric and kinematic parameters for the pinion finishing operation. Int J Adv Manuf Technol 32:1170–1187. doi:10.1007/s00170-006-0439-0
5. Bianco G (2000) Gear shaving. Jiuge, Beijing
6. Litvin FL (1994) Gear geometry and applied theory. PTR Prentice Hall, New Jersey
7. Chang SL, Lin HJ, Chu CH, Liu JH, Hung CH (2007) Simulation of gear shaving machine and tooth contact analysis of the shaved gears. Proc IAENG Int Conf Ind Eng 2:2187–2192
8. Hung CH, Liu JH, Chang SL, Lin HJ (2007) Simulation of gear shaving with considerations of cutter assembly errors and machine setting parameters. Int J Adv Manuf Technol 35(3–4):400–407. doi:10.1007/s00170-007-1176-8
9. Litvin FL, Fan Q, Vecchiato D, Demenego A, Handschuh RF, Sep TM (2001) Computerized generation and simulation of meshing of modified spur and helical gears manufactured by shaving. Comput Methods Appl Mech Eng 190:5037–5055. doi:10.1016/S0045-7825(00)00362-5
10. Koga H, Umezawa K, Miao HC (1996) Analysis of plunge shaving process for helical gears with tooth modifications. Power Transmission and Gearing Conference, San Diego, CA, vol. 88, pp 265–273
11. Hsu RH (2006) Theoretical and practical investigations on the design of plunge shaving cutter. Ph.D. Dissertation, National Chung Cheng University.
12. Radzevich SP (2003) Design of shaving cutter for plunge shaving a topologically modified involute pinion. J Mech Des 125:632–639. doi:10.1115/1.1588346
13. Radzevich SP (2005) Computation of parameters of a form grinding wheel for grinding of shaving cutter for plunge shaving of topologically modified involute pinion. J Mech Des 127:819–828
14. Piegl L, Tiller W (1997) The NURBS Book, 2nd edn. Springer-Verlog, Berlin
15. Wang F, Yi C, Wang T, Yang S, Zhao G (2005) A generating method for digital gear tooth surfaces. Int J Adv Manuf Technol 28:474–485. doi:10.1007/s00170-004-2395-x
16. Barone S (2001) Gear geometric design by B-spline curve fitting and sweep surface modeling. Eng Comput 17:66–74. doi:10.1007/s003660170024